*Applied Chemical Engineering (2025) Volume 8 Issue 4* ISSN: 2578-2010 (O)
doi: 10.59429/ace.v8i4.5804

**ORIGINAL RESEARCH ARTICLE**

# A study of the process of evaporation of mother liquors formed during the production of double salts of glaserite and schoenite

**Nafisa Ulasheva[1], Bakhrom Kucharov[1], Aktam Erkaev[2], Bakhtiyor Zakirov[1], Mashkhurakhon Yulbarsova[1], Davron Isabaev[1], Erkin Israilov[1], Surayyo Jumadullaeva[1], Gulnar Saparova[3], Atabek Kaipbergenov[3], Karjaubay Reymov[4], Sardor Sherkulov[5], Aziz Dustov[5], Odil Nazarov[5], Kakhramon Turayev[6], Bakhodir Abdullayev[5*]**

[1]*Institute of General and Inorganic Chemistry of the Academy of Sciences of the Republic of Uzbekistan, Tashkent, 100170, Uzbekistan*

[2]*Tashkent Institute of Chemical Technology (TICT), Tashkent, 100011, Uzbekistan*

[3]*Nukus State Technical University, Nukus, 230100, Karakalpakstan*

[4]*Nukus State Pedagogical Institute, Nukus, 230100, Karakalpakstan*

[5]*University of Economics and Pedagogy, Karshi, 180119, Uzbekistan*

[6]*Karshi State Technical University, Karshi, 180119, Uzbekistan*

***Corresponding author:** Bakhodir Abdullayev, bahodir.abdullayev.92@mail.ru

## ABSTRACT

This article presents data on the synthesis process of glaserite and schoenite through a two-stage transformation of astrakhanite. The first stage involves the initial conversion of astrakhanite, followed by a secondary transformation aimed at producing potassium sulfate. To facilitate the separation of sodium chloride and enhance the yield of potassium chloride in the final products, the evaporation behaviour of glaserite and schoenite mother liquors was investigated. During glaserite mother liquor evaporation, filtration at elevated temperatures results in the near-complete crystallisation of sodium chloride, while filtration at low temperatures almost entirely facilitates the crystallisation of mirabilite. This creates the potential for successful sodium chloride separation from the mother liquor and the creation of positive conditions for potassium sulfate recovery enhancement in the subsequent process steps. For the schoenite mother liquor, hot filtration following the evaporation leads to the solid phase being approximately 33.5% schoenite, 1.7% arcanite, 56.0% bischofite, 7.9% magnesium sulfate, and 11.8% unknown crystalline phases. The solid phase composition at the cold condition is significantly different from that of schoenite and arcanite, increasing to 54.8% and 27.6%, respectively. It is established that the solid material obtained by hot filtration of the schoenite mother solution is fit for the purposes in the processes of bischofite manufacturing, and the precipitate obtained by cold filtration can be used directly in the form of ready-to-use fertiliser.

***Keywords:*** glaserite; schoenite; conversion; potassium chloride; evaporation

**ARTICLE INFO**

Received: 11 October 2024
Accepted: 24 November 2025
Available online: 05 December 2025

## 1. Introduction

Today, Potassium fertilisers contribute significantly to global food security through increased crop productivity and the enhancement of stress-tolerant agricultural systems. By 2023, potassium fertiliser consumption across the globe had attained about 44.2 million metric tons in terms of 100% $K_2O$. This consumption is projected to increase to 46 million tons between 2025 and 2028 due to factors like climate change and the growth in the human population, with the consequent enhancement of agricultural productivity [1-5].

The leading potassium fertiliser-producing nations in the 2023-2024 period were Canada, Russia, Belarus, the United States, and

Jordan. Huge consumption also originated in China, Brazil, India, and Indonesia. Muriate of potash (potassium chloride, KCl) is the most popular potassium fertiliser in modern agricultural practice throughout the world. The application of fertilisers that contain chloride is much restricted for the sensitive-to-chloride crops like sugar beet, potatoes, and citrus in particular. Nevertheless, in some protected growing situations, it may be imperative to utilise the fertilisers with the base of the chloride [6-9].

For chloride-sensitive crops, the alternative of choice is potassium sulfate ($K_2SO_4$), which makes up about 10% of the world's total potassium fertiliser output [10-11].

The potassium sulfate production could be widely framed under two methodological procedures:

Processes with potassium chloride (KCl) employed as the potassium-source material that is chemically converted with sulfuric acid, sodium sulfate, or ammonium sulfate to yield potassium sulfate in double decomposition or conversion reactions [12].

Processes that employ naturally occurring mineral sources such as polyhalite ($K_2SO_4 \cdot MgSO_4 \cdot 2CaSO_4 \cdot 2H_2O$) and langbeinite ($K_2SO_4 \cdot 2MgSO_4$) as raw materials [13].

Moreover, methods for converting phosphogypsum into chloride-free potassium fertilisers have also been developed. They entail treatment with potassium carbonate, or with potassium chloride directly or with an intermediate treatment with ammonium sulfate. Not least practical importance is the straight conversion of potassium chloride and phosphogypsum to potassium sulfate or syngenite ($K_2SO_4 \cdot CaSO_4 \cdot H_2O$), providing an effective route to the synthesis of fertilisers free of chloride.

## 2. Materials and methods

The synthesis of glaserite was done in accordance with the data measured from the $Na_2SO_4$–$MgSO_4$–KCl system plane section found in the $2Na^+$, $2K^+$, $Mg^{2+}$ // $SO_4^{2-}$, $2Cl^-$ – $H_2O$ diagram at 75 °C. From this section, it is found that at 75°C, the ratio between potassium chloride and astrakhanite was 25.86/74.14, resulting in the formation of a solution at point $A_2^{75}$ and a solid phase that was separated from the liquid phase. The schonite was synthesised using data from the $2Na^+$, $2K^+$, $Mg^{2+}$ // $SO_4^{2-}$, $Cl^-$ – $H_2O$ diagram section of the $Na_2SO_4$–$MgSO_4$–KCl system at 0°C. At 0°C, at the solubility point $A_1^0$, mixed solutions are formed with crystallisation of mirabilite and schonite. Thus, for synthesis, mother liquor from the preparation of glaserite at point $A_2^{75}$ was used. At 0 °C, composition $A_2^0$ is within the region of crystallisation of schonite, and then a measured amount of potassium chloride was added to this solution at $A_3^0$. This resultant solution was cooled to 0 °C, leading to the formation of crystals of schonite with composition $K_2SO_4 \cdot MgSO_4 \cdot 6H_2O$. The concentration of chloride ions was measured by Mohr's method. Sodium and potassium ion concentrations were measured by a single-channel flame photometer, model PFP7/C, a low-temperature instrument for clinical estimation of sodium, potassium, and lithium. PFP7/C's in-built linearization circuitry gives direct read-outs of potassium and sodium concentrations in mol/L. The XRD was performed using an XRD-6100 diffractometer (Shimadzu, Japan) interfaced to a computer. CuKα radiation was employed under the following parameters: 30 mA and 30 kV current and voltage, respectively; detector rotation rate of 4°/min with a step size of 0.02°, and scanning angle range (2θ) of 4° to 80°.

## 3. Results and discussion

The aim of the present research work is the synthesis of glaserite and schoenite by a two-stage conversion technique, where the precursor compound is astrakhanite. This technique includes the preliminary conversion of astrakhanite and a subsequent conversion for the synthesis of potassium sulfate ($K_2SO_4$). The work also examines the conversion of the mother liquors that result when synthesising glaserite and schoenite for purposes of recuperating potassium sulfate, an agriculturally important and crucially scarce fertiliser. The composition of the filtrates is shown in Table 1. For enhanced segregation between sodium chloride and increased yield of potassium chloride in the final product, the evaporation behaviour of the glaserite and schoenite mother liquors has been studied in detail.

**Table 1.** Elemental composition of the liquid phase after conversion (g/l).

| The measurement range of a particular element | Na | Mg | P | K | Cr | Fe | Ni | Cu | Zn | Br |
|---|---|---|---|---|---|---|---|---|---|---|
| Glaserite | >1000 | 470 | 9.3 | 310 | 2 | 1.3 | 0.13 | 0.3 | 5.9 | 12 |
| Schoenite | 810 | >5000 | 12 | 200 | 2.7 | 2 | 0.56 | 0.11 | 3.4 | 13 |

The results of the evaporation experiments conducted on the mother liquor are summarised in Tables 2 and 3. A look at the data in Table 2 indicates that while the evaporation degree increases from 10% to 40%, the liquid-to-solid ratio significantly reduces from 20:1 and 40:1 to 0.487:1 and 2.89:1 for the conditions of hot and cold filtration, respectively. This trend corresponds to an increase in the forming precipitate: for conditions of higher temperature, the solid phase increases from 4.04% to 38.28%, while for conditions of lower temperature, it increases from 1.82% to 4.04% relative to the initial total weight of the system.

It is notable that for evaporation rates between 10% and 30%, the amount of precipitate so-formed under both sets of thermal conditions is nearly the same. However, when the evaporation is 40%, the amount of solid so-formed under the higher temperatures exceeds that so-formed in the lower temperatures by a factor larger than nine. Correspondingly, the moisture content of the precipitate reduces from 20.11% to 11.11% with the increase of the level of evaporation and oscillates in the range between 11.11% and 33.3%. Additionally, the filtration rate exceeds 266.37 kg/m$^2$·h (as indicated in Table 2).

**Table 2.** Study of the process of evaporation of mother liquors during the production of glaserite

| **Degree of evaporation, %** | **L:S ratio** | | **Yield of the solid phase relative to the total initial mass of the system, %** | | **Sediment moisture content, %** | | **Filtration rate, kg/m$^2$ h** | |
|---|---|---|---|---|---|---|---|---|
| | In a hot state | In a cold state | In a hot state | In a cold state | In a hot state | In a cold state | In a hot state | In a cold state |
| 10 | 20:1 | 40:1 | 4.09 | 1.82 | 33.30 | 20.11 | 50.43 | 454.03 |
| 20 | 14.44:1 | 15.89:1 | 4.91 | 4.09 | 24.07 | 23.81 | 64.46 | 438.45 |
| 30 | 9.14:1 | 10.78:1 | 6.36 | 4.54 | 21.43 | 30.02 | 222.78 | 410.86 |
| 40 | 0.487:1 | 2.89:1 | 38.28 | 4.09 | 21.62 | 11.11 | 266.37 | 431.34 |

Figure 1 will show that the resultant solid phase is predominantly sodium chloride, which accounts for more than 55% of the overall initial mass, and thenardite ($Na_2SO_4$) accounts for 41.0% of the overall initial mass. The overall yield for these compounds is near 96% for the initial mass of the system.

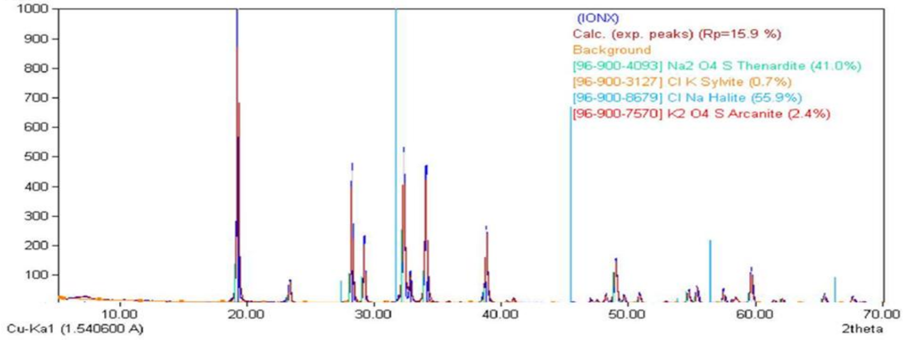

**Figure 1.** X-ray phase analysis of the precipitate formed during evaporation of glaserite mother liquor in a hot state

Figure 2 below shows an elemental analysis of the solid phase. It shows that a mixture of mirabilite and thenardite precipitates under cold conditions in amounts below 40% of the evaporation level.

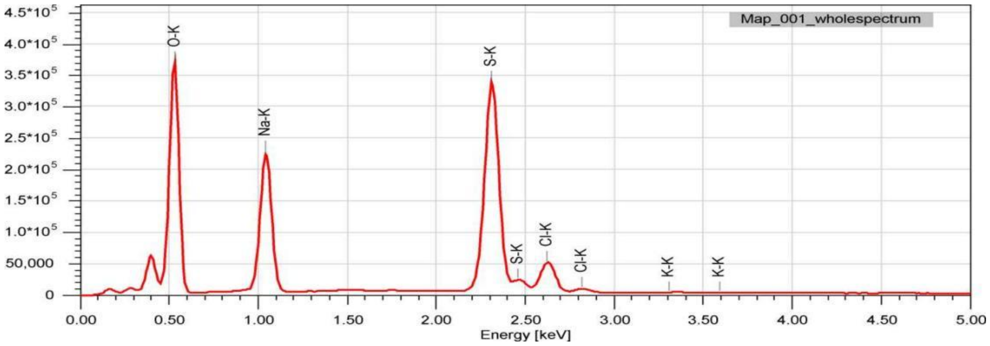

**Figure 2.** Diagnostics Expression of syphilis by analysis of the sediment formed during evaporation of 40% mirabilite and thenardite in the cold

Figure 3 shows that the particle size ranges from 30-90 µm, with an uneven, angular surface. In the second image, the particle size ranges from 45-70 µm, with a smooth surface and a well-defined crystalline structure.

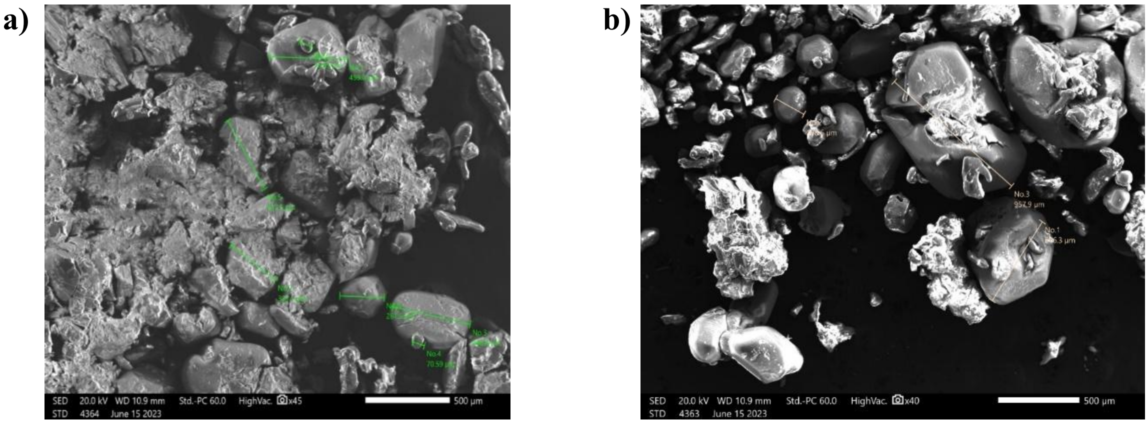

**Figure 3.** SEM analysis of mirabilite (a) and thenardite(b) crystals.

Table 3 shows the results of mother liquor evaporation after separation of the schoenite precipitates. Table 4 shows that after 50% evaporation, the solid phase begins to precipitate. As the evaporation degree increases from 55 to 70%, the L:S ratio decreases from 11.71 to 12.21 and to 1.47:1 and 0:1, respectively. That is, at 70% evaporation with cooling below 300°C, the mass completely solidifies. The moisture content of the precipitates ranges from 13.81 to 18.18%, and the filtration rate is low, amounting to 196.24 to 331.22 kg/m²·h.

**Table 3.** Study of the process of evaporation of mother liquors during the production of glaserite

| **Samples** | **Degree of evaporation, %** | **L:S ratio** | | **Yield of the solid phase relative to the total initial mass of the system, %** | | **Sediment moisture content, %** | | **Filtration rate, kg/m² h** | |
|---|---|---|---|---|---|---|---|---|---|
| | | In a hot state | In a cold state | In a hot state | In a cold state | In a hot state | In a cold state | In a hot state | In a cold state |
| 1 | 10 | 63:0 | – | – | – | – | – | – | – |
| 2 | 20 | 56:0 | – | – | – | – | – | – | – |
| 3 | 30 | 48:0 | – | – | – | – | – | – | – |
| 4 | 40 | 42:0 | – | – | – | – | – | – | – |

| Samples | Degree of evaporation, % | L:S ratio | | Yield of the solid phase relative to the total initial mass of the system, % | | Sediment moisture content, % | | Filtration rate, kg/m$^2$ h | |
|---|---|---|---|---|---|---|---|---|---|
| 5 | 50 | 11.71:1 | 12.21:1 | – | – | – | – | – | – |
| 6 | 55 | 4:1 | 2.45:1 | 7,87 | 7,57 | 14,84 | 16,28 | 263,24 | 196,94 |
| 7 | 60 | 2.49:1 | 1.01:1 | 28,64 | 14,27 | 13,81 | 18,18 | 331,27 | 261,171 |
| 8 | 70 | 1.47:1 | – | 40,45 | – | 15,79 | – | 243,58 | – |

**Table 3.** (*Continued*)

Figure 4 presents the results of the TGA and DTA analyses of the precipitates obtained within the temperature range from 0 to 800 °C. The DTA curve exhibits three endothermic effects at 126.08 °C, 365.01 °C, and 451.79 °C, as well as one exothermic effect at 240.9 °C.

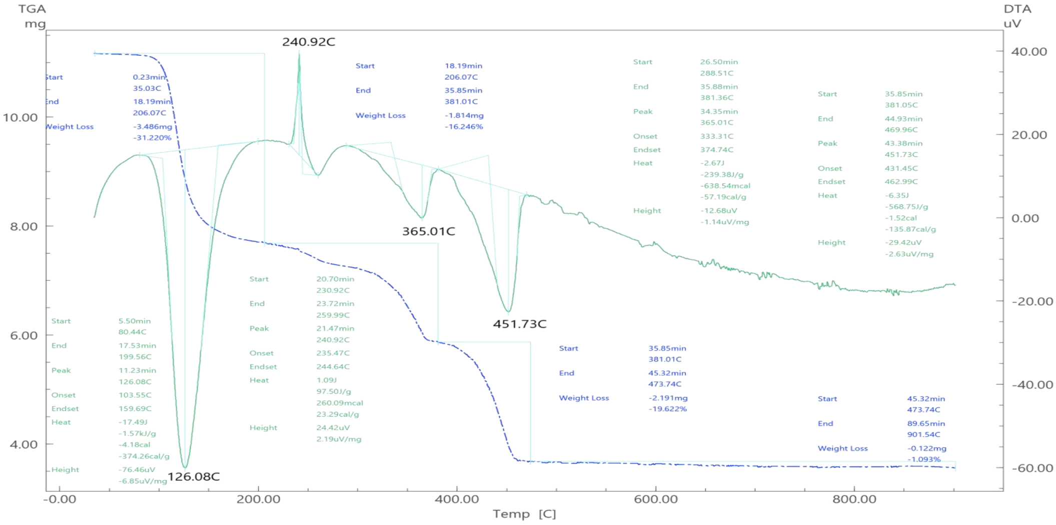

**Figure 4.** DTA and TGA of the solid phase formed under the synthesis conditions

According to the data from the TGA and illustrated in Table 4, the greatest mass loss occurs at the first endothermic peak that happens in the temperature range from 80.44 to 199.56 °C, in which the mass loss exceeds 31.22%. In the second and third succeeding endothermic peaks, the mass losses detected are 16.25% and 19.62%, respectively. The exothermic peak detected at the temperature value of 240.92 °C does not yield any remarkable mass loss, which is likely attributed to the crystalline phase in the mineral constituents undergoing polymorphic transformation.

The amount of energy consumed in the process of endothermic reactions directly corresponds with the mass decrease, which was measured at 570 J/g, 239.38 J/g, and 568.7 J/g, respectively. On the other hand, the energy released in exothermic reactions often decreases considerably, from a factor of roughly 2.5 to 17 to only 97.5.

**Table 4.** Study of the process of evaporation of mother liquors during the production of glaserite

| The nature of the thermal effect | The beginning of the effect | | End of effect | | Peak effect | | Specific heat, J/g | Weight loss, % | | | | |
|---|---|---|---|---|---|---|---|---|---|---|---|---|
| | | | | | | | | Start | | End | | % |
| | τ | T, °C | τ | T, °C | τ | T, °C | | τ | T, °C | τ | T, °C | |
| Endothermic | 63:0 | 5.50 | 80.44 | 17.53 | 199.56 | 11,23 | 126.08 | -1570 | 0.23 | 35.03 | 18.19 | 206.07 |
| Exothermic | 56:0 | 20.70 | 230.92 | 23.72 | 259.99 | 21.47 | 240.92 | 97.50 | 18.19 | 206.07 | 35.85 | 381.01 |

| The nature of the thermal effect | The beginning of the effect | | End of effect | | Peak effect | | Specific heat, J/g | Weight loss, % | | | | |
|---|---|---|---|---|---|---|---|---|---|---|---|---|
| | | | | | | | | Start | | End | | % |
| | τ | T, °C | τ | T, °C | τ | T, °C | | τ | T, °C | τ | T, °C | |
| Endothermic | 48:0 | 26.50 | 288.51 | 35.88 | 381.36 | 34.35 | 365.01 | -239.38 | 35.85 | 381.01 | 45.32 | 473.74 |
| Endothermic | 42:0 | 35.85 | 381.05 | 44.93 | 469.96 | 43.38 | 451.73 | -568.75 | 45.32 | 473.74 | 89.65 | 901.54 |

**Table 4.** (*Continued*)

At the 60% degree of evaporation, the precipitate solid phase totals 7.87% and 7.57% under hot and cold conditions, respectively. Shown in Figures 5 and 6, the hot conditions at 60% evaporation in the solid phase are comprised of 33.5% schoenite, 1.7% arcanite, 56.0% bischofite, 7.9% magnesium sulfate, and 11.8% unknown peaks. In the cold conditions, the total content in the solid phase becomes higher and the schoenite and the arcanite total 54.8% and 27.6%, respectively. The dimensions of the crystals range from 33.55 to 251.3 µm, see Fig. 7.

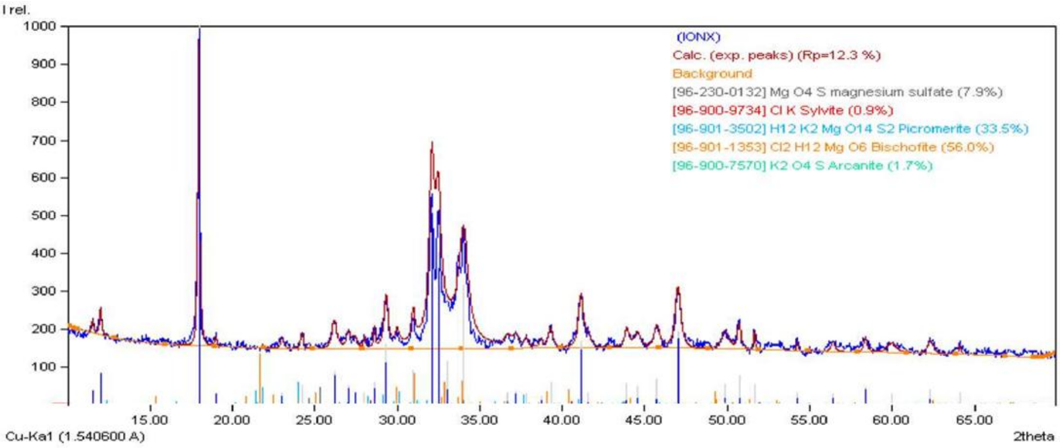

**Figure 5.** X-ray diffraction pattern of precipitates formed in a hot state at 60% evaporation

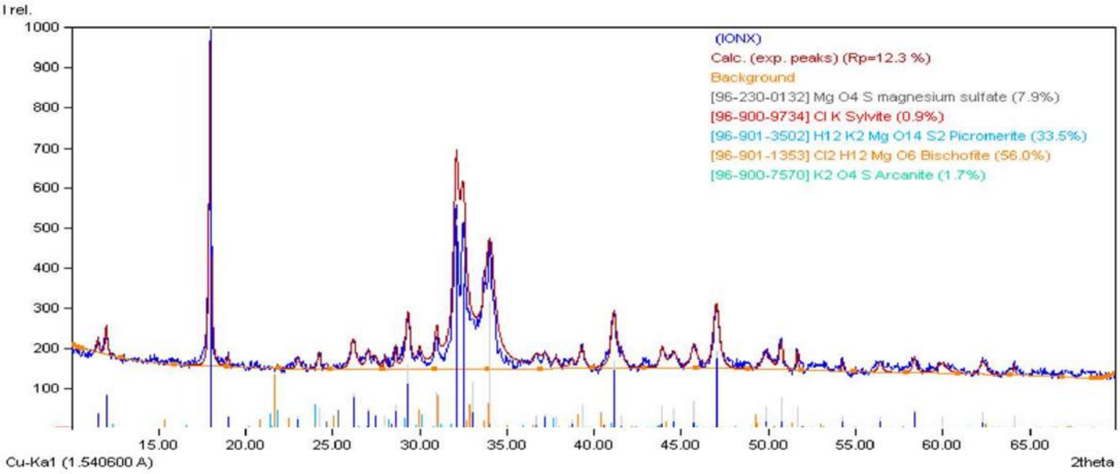

**Figure 6.** X-ray diffraction pattern of precipitates formed in a cold state at 60% evaporation

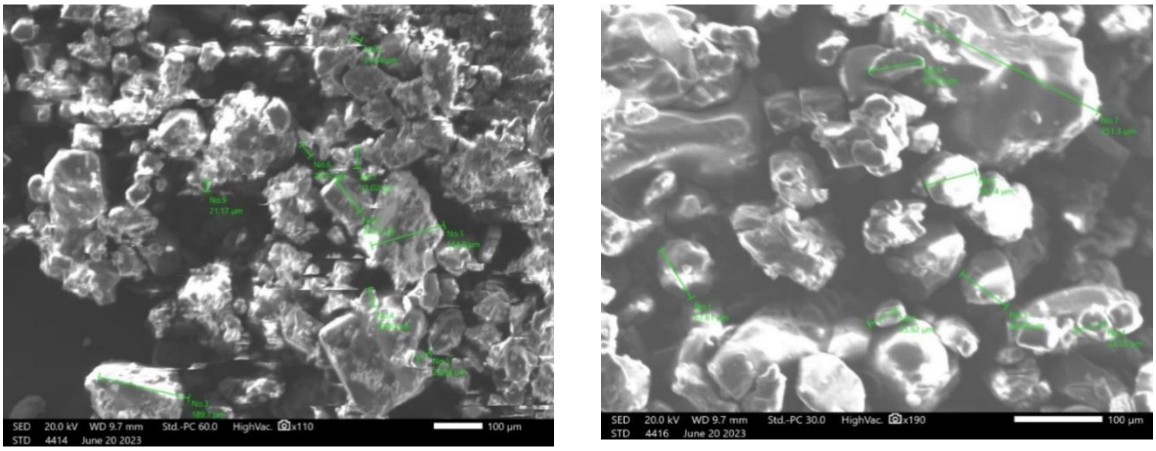

**Figure 7.** SEM analysis of sediments at 60% evaporation in a cold state (33.55 to 251.3 µm)

Experimental data show that after separating the precipitates, magnesium hexahydrate precipitates in the remaining liquid phase during storage and the Mg content in the filtrate decreases by 5-7 times compared to the original mother liquor. The size of the precipitated crystals ranges from 360.7 to 1098 µm.

## 4. Conclusion

The evaporation behaviour of mother liquors containing glaserite and schoenite offers effective strategies for enhancing $K_2SO_4$ recovery through multi-step conversion processes. In glaserite systems, hot-state evaporation facilitates the removal of approximately 96% of sodium salts, primarily NaCl and thenardite, thereby improving the selectivity and efficiency of subsequent crystallization. While cold evaporation yields lower solid output, it aids in mirabilite formation and selective $Na_2SO_4$ separation, though hot filtration remains superior for upstream purification.

For schoenite-rich liquors, cold filtration after 60% evaporation results in solids with higher $K_2SO_4$ content up to 82.4% comprising both schoenite and arcanite, outperforming hot filtration in potassium salt yield. Additionally, magnesium impurities in the residual solution can be reduced 5-7-fold via $MgSO_4 \cdot 6H_2O$ precipitation.

Process optimization focuses on stage-controlled evaporation, ideally 30-40% for glaserite and 55-60% for schoenite, temperature-specific filtration (hot for NaCl, cold for $K_2SO_4$), and sequential impurity removal by ageing to crystallize magnesium salts. High filtration rates (266.37 $kg/m^2 \cdot h$ for glaserite and 331.27 $kg/m^2 \cdot h$ for schoenite) demonstrate large-scale feasibility. However, challenges remain in temperature regulation and premature crystallization control. Overall, controlled evaporation and temperature-adjusted filtration significantly enhance $K_2SO_4$ recovery while supporting sodium and magnesium salt separation and diverse product output.

## Author contributions

Nafisa Ulasheva: Conceptualization, methodology, investigation, writing- original draft; Bakhodir Abdullayev: Visualization, project administration, writing-reviewing and editing; Bakhrom Kucharov, Aktam Erkaev: Supervision, visualization, project administration, writing-reviewing and editing, reformatting, grammar editing; Bakhtiyor Zakirov, Mashkhurakhon Yulbarsova, Abror Aliev, Davron Isabaev, Erkin Israilov, Surrayo Jumadullaeva, Gulnar Saparova, Atabek Kaipbergenov, Karjaubay Reymov, Sardor Sherkulov, Odil Nazarov, Aziz Dustov, Kakhramon Turayev: Investigation and resource.

## Fundings

No fundings

## Acknowledgments

The authors would like to thank all those who contributed to this study and worked on its development.

## Conflict of interest

The authors declare no conflict of interest.

## References

1. Penuelas, J., Coello, F., Sardans, J. A better use of fertilizers is needed for global food security and environmental sustainability. Agriculture & Food Security 2023; 12(1), 1-9. https://doi.org/10.1186/s40066-023-00409-5
2. Sinha, D., Tandon, P.K. An overview of nitrogen, phosphorus and potassium: Key players of nutrition process in plants. Sustainable solutions for elemental deficiency and excess in crop plants2020;85-117. https://doi.org/10.1007/978-981-15-8636-1_5
3. Römheld, V., Kirkby, E.A. Research on potassium in agriculture: needs and prospects. Plant and soil 2010; 335(1), 155-180. https://doi.org/10.1007/s11104-010-0520-1
4. White, P.J. Improving potassium acquisition and utilisation by crop plants. Journal of Plant Nutrition and Soil Science 2013; 176(3), 305-316. https://doi.org/10.1002/jpln.201200121
5. Sardans, J., Peñuelas, J. Potassium control of plant functions: Ecological and agricultural implications. Plants 2021; 10(2), 419. https://doi.org/10.3390/plants10020419
6. Al Rawashdeh, R. World peak potash: An analytical study. Resources Policy 2020; 69, 101834. https://doi.org/10.1016/j.resourpol.2020.101834
7. Abdullayev, B., Makhmayorov, J., Ro‘ziyeva, Z., Shabarova, U., Deng, T., Samadiy, M. Study of the mutual influence of components in the lithium nitrate–ammonium chloride–water system. New Materials, Compounds and Applications 2023; 7(3), 188-193.
8. Nguyen, T.H., Tang, F.H., Conchedda, G., Casse, L., Obli-Laryea, G., Tubiello, F.N., Maggi, F. NPKGRIDS: a global georeferenced dataset of N, $P_2O_5$, and $K_2O$ fertilizer application rates for 173 crops. Scientific Data 2024; 11, 1179. https://doi.org/10.1038/s41597-024-04030-4
9. Singh, N., Maurya, V., Gupta, K., Sharma, I., Sharma, A., Kumar, R. Salt stress and its eco-friendly management using biostimulants in grain legumes: a review. Discover Agriculture 2025; 3(1), 13. https://doi.org/10.1007/s44279-024-00150-y
10. Abdullayev, B., Rakhimov, M., Borikhonov, B., Dustov, A., Samadiy, M. Study of the mutual influence of components in the system potassium sulfate-lithium sulfate-water. AIP Conference Proceedings 2024;3184(1), 020012. https://doi.org/10.1063/5.0212016
11. Wang, Q., Shan, C., Zhang, P., Zhao, W., Zhu, G., Sun, Y., Wang, Q., Jiang Y., Shakoor, N., & Rui, Y. The combination of nanotechnology and potassium: applications in agriculture. Environmental Science and Pollution Research 2024; 31(2), 1890-1906. https://doi.org/10.1007/s11356-023-31207-y
12. Yin, Z., Li, Y., Guo, H., Liu, X., Cao, J. Research on the $K_2SO_4$ Synthesis Process Based on the Nonequilibrium-Phase Diagram of the $Na^+$, $K^+$//$Cl^-$, $SO_4^{2-}$–$H_2O$ System. Industrial & Engineering Chemistry Research 2025; 64(26), 13277-13288. https://doi.org/10.1021/acs.iecr.5c00555
13. Ma, F., Zeng, Y., Yu, X., Chen, K., Ren, S. The Leaching Behavior of Potassium Extraction from Polyhalite Ore in Water. ACS Omega 2023; 8(40), 37162-37175. https://doi: 10.1021/acsomega.3c04733